RESEARCH PAPER

Nanoformulation and Biological Evaluation of Kaempferol Nanoparticles for Enhanced Antibacterial Activity

Wisam Mahmood Mohammed [1]*, *Aws K. Mohammed* [2], *Ahmed M. Shano* [3]

[1] *Ministry of Education, Open Educational College, Iraq*

[2] *Ministry of Education,General Directorate of Education in Diyala, Iraq*

[2] *Department of Radiological Techniques, Bilad Alrafidain University College, Diyala, Iraq*

ARTICLE INFO

Article History:
Received 19 December 2025
Accepted 28 March 2026
Published 01 April 2026

Keywords:
Biological activity
Chitosan
Kaempferol
Nanoformulation

ABSTRACT

The work involved prepare and characterization of new derivatives nanoparticles of Kaempferol with chitosan that produced by hydrothermal method, FTIR used to characterized these compounds. XRD analysis clarified the amorphous structure of the nanoparticles samples, AFM gave an average diameter (62.99, 75.31, 91.37) nm of (copper, iron oxide) Schiff base –g- Kaempferol coated respectively, and SEM results gave a clear agglomeration of the material biological activity study against four type of bacteria and two types of antifungals.

How to cite this article
Mohammed W., Mohammed A., Shano A. Nanoformulation and Biological Evaluation of Kaempferol Nanoparticles for Enhanced Antibacterial Activity. J Nanostruct, 2026; 16(2):2078-2086. DOI: 10.22052/JNS.2026.02.054

INTRODUCTION

Specific chemicals and/or plant extracts obtained from natural sources (containing various secondary metabolites) have been proven to have antioxidant action. Plant metabolites have long acts as a means of inspiration for medicinal chemists and a platform for drug development They can play a series of ecological roles in the plant, including protecting it against herbivores, fungus, bacteria, and viruses, as well as assisting it in competing for water, light, and nutrients. [1] Kaempferol (3,4',5,7-tetrahydroxyflavone) is a flavonoid found in kale, beans, tea, spinach, and broccoli, among other plants and plant derived foods. Kaempferol is a yellow crystalline substance that melts at 276–278 degrees Celsius (529–532 degrees Fahrenheit). It is soluble in hot ethanol, ethers, and DMSO but very slightly in water [2]. Because kaempferol's structure is similar to estrogen's, it could have both estrogenic and antiestrogenic effects depending on its concentration, and it could be used to treat hormonal cancers like ovarian, breast, and cervical cancers, as well as hepatocellular carcinoma, acute promyelocytic leukemia, and glioma. [3-4] There are four key stages in the production of kaempferol. In the first phase, phenylalanine is transformed into 4-coumaroylCoA via the phenylpropanoid metabolic pathway. Through the activity of chalcone synthase, 4-coumaroyl-CoA is joined with three molecules of malonyl coA to create naringenin chalcone (a tetrahydroxychalcone). The hydroxyl group of naringenin chalcone is implicated in the production of dihydrokaempferol in the third stage, when it is swapped with naringenin. Finally,

* *Corresponding Author Email: mahmoodwisam737@gmail.com*

dihydrokaempferol is transformed to kaempferol, which possesses a double bond [5-6].

About biomedical applications, the nanoparticles are almost surface modified. Furthermore, the modification can increase the chemical stability of the nanoparticles. An assortment of materials coating to modify the metal nanoparticles, like silica or biopolymers or until carbon [7-9]. This surface coating is important to avoid oxidation and the nanoparticles agglomerate, which increases their biocompatibility [10] in biomedical applications Fe_3O_4 NPs can be used in drug delivery magnetic resonance imaging (MRI), contrast agents and therapy [11-12]. There are several methods of synthesizing magnetite nanoparticles. The most common method is the co-precipitation of ferrous and ferric ions into an alkaline medium [13]. In addition, thermal decomposition [14], sol-gel synthesis [15], hydrothermal synthesis [16], electrochemical synthesis [17] and microwave assisted synthesis [18]. Recently, studies have shown that the incorporation of copper nanoparticles into chitosan significantly reinforce its antimicrobial and antifungal activity [19]. The choice of chitosan as a stabilizer for Cu NPs due to its ability to chelate metals, making it an ideal material for metal nanoparticles. Chitosan as a stabilizer and or reducing agent [20].

MATERIALS AND METHODS

Materials

Chitosan (code KB-002) (Merck) (Deacetylation content=89%), kaempferol locally. Propanaldyhede (Sigma-Aldrich) Succinic Anhydride (BDH).

Instrumentals

FTIR spectra were recorded in KBr discs on (FTIR model 8000) Testcan Shimadzu IR-Spectrometer under dry air at room temperature within the wave number range of 4000-600 cm^{-1}.Samples were heated from 0 to 500 °C in a platinum pan with a heating rate 10 °C / min, in N2 atmosphere of flow rate 25 mL / min. X-ray diffraction technique Research Center, Baghdad (Shimadzu 6000 X-ray with 2θ angle covered from 20 to 80 degree) The roughness of the nanoparticles surface was characterized using AFM (type AT3000, Angstrom, Scanning Probe Microscope, Advanced Inc., USA). This technique provides two- and three-dimensional profile images. Scanning electron microscopy of nanoparticles were determined by (TESCAN-Czech Republic).

Extraction

The separation of medicinally active parts of plant or animal tissues from inactive or inert components using selected solvents in conventional extraction techniques is referred to as extraction in the pharmaceutical industry. Plant-derived products are impure liquids, semisolids, or powders intended for oral or external use alone. [21]. Aligi (kaempferol) , was weighed (100 g) and put in a beaker with (1000 ml) of 70 % ethanol. The solution is macerated for 48 h at room temperature with 360 rpm agitation until the soluble stuff has dissolved. The solution was purified by filtering under vacuum using filter paper after maceration, and then concentrated using a rotary evaporator (less than 70°C under decreased pressure). Finally, the extracted material was weighed and placed in the refrigerator to be analyzed later [22].

Methods

Preparation ofpoly Schiff base of chitosan (Ch-Pr) (1) [23]

A (1 gm) of chitosan in (50 ml) of glacial acetic acid (1%) was stirred at 30 °C for 1 h. A (0.009mol,0.52 g) of propanaldehyde mixed with chitosan The mixture was stirred and heated in a water bath at 70 °C for 6 h. 5% sodium hydroxide drops are added until precipitation of the desired compound. The Transparent white precipitate was collected and washed with (10 ml) diethyl ether and to remove any remaining materials. The products were filtered and dried in a vacuum oven at 60 °C overnight [24].

Synthesis of (chitosan– grafted - kaempferol) (2)

An amount of 0.007mol, 2 g of kaempferol was dissolved in absolute ethanol, added to 3 g of chitosan-g-succinic anhydride that had been dissolved in 10 ml of dimethyl sulfoxide (DMSO), and the mixture was refluxed for 6 hours at 70 °C. The black precipitate was collected, continuously washed with 10 ml of di-ethyl ether, and then dried in a vacuum oven at 50 °C [26].

Preparation of Schiff base–grafted-kaempferol-coated Cu NPs (3)

Copper-chitosan Schiff base nanoparticles synthesized by green method via one-step which is 1gr Schiff base – grafted - kaempferol dissolved in 50 ml of ethanol then add 25 ml of (0.3g) copper sulfate ($CuSO_4.5H_2O$) and stir in 70 °C for 13 hours until a reaction, is complete. After then, 13 hours a

result product centrifuged in 5000 G to30 minutes till particles are separate from suspension. Resupended the precipitat in acetone (99% $^{v}/_{v}$) then the centrifugation has been reiterated five times to co-precipitation.

Preparation of Schiff base – grafted - kaempferol -coated Fe NPs (4)

Magnetite iron oxide (Fe_3O_4) nanoparticles are prepared via the co-precipitation, method which $FeCl_3.6H_2O$ and, $FeCl_2.4H_2O$, which include (1.7g) and (4.7g) respectively of salts in 50 ml deionized water. Then ammonia solution (25%) has been added to the salts of iron solution meanwhile syringe pump beneath mechanical stirring until the pH of the solution arrive to ± 10. In the precedent process will generate the dark brown precipitant of Fe3O4 nanoparticles. The generated precipitant washing in deionized water to eliminate every alkali metals and until arrive the solution (pH±7). The resulting product dried via freeze process. To synthesize Fe_3O_4 nanoparticles coated chitosan –g-kamferol then added to it and was heated at 70 ºC for 2 hours to output a transparent solution which is known "sol". The obtained sol has been heated to evaporate most of its solvent and getting an additional viscous gel [27,28].

Antimicrobial activity [29]

Antibacterial activity of the prepared compounds was evaluated against types of bacteria (Gram-positive and Gram-negative), *Streptococcus, Bacillus, Escherichia coli, Klebsiella* the testing was performed using Agar diffusion method. The inhibition zone is measured by using a metric ruler over the inhibition zone, at its widest diameter, and then measuring from one edge of the zone to the other. It may be helpful to hold the panel up to the light and then use measurements in millimeters. Most of the tested compounds showed clear antibacterial activity, especially compound 1,2 the results of these two compounds were nearly similar to those of Ampicillin, which was used as a reference. Compound 5 showed the greatest activity against bacteria *Bacillus, Candida.* While compound 3 showed the strongest effect against *Candida* and both compounds had a strong effect against other bacteria. While compound 4

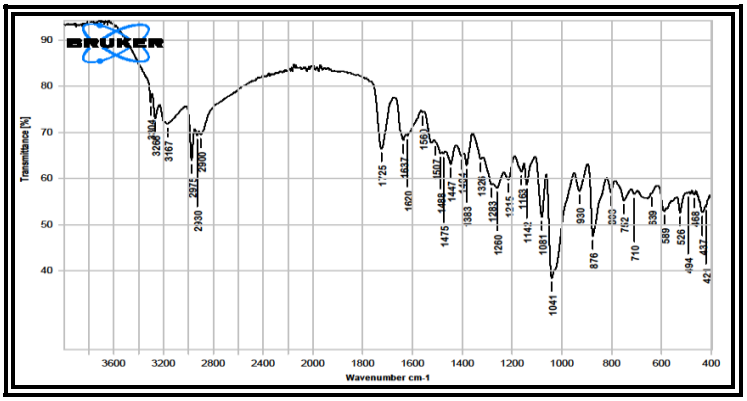

Fig. 1. FTIR spectra of compound of 1.

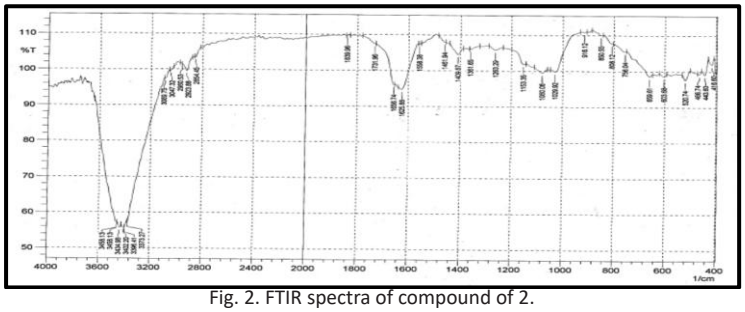

Fig. 2. FTIR spectra of compound of 2.

showed the strongest effect against *Candida* and both compounds had a strong effect against other bacteria.

RESULT AND DISCUSSION

This study includes synthesis and polymerization of new derivative compounds of nanoparticles of kaempferol and Schiff base through the reaction of amin groups in chitosan with propanaldehyde then Schiff base reaction with succinic anhydride by ring opening the carboxylic groups in succinate reaction with hydroxyl group in kaempferol.

FTIR

The infrared spectra of the compounds are presented in Figs.1-3. It was shown that a high intensity band at the range of (3379-3480) cm^{-1} which refer to the stretching vibrations of hydroxyl groups. Moreover, the high intensity of this band due to the presence of more than two hydroxyl groups in the structure of these compounds. The spectra of compounds (1-3) show two bands at (3000-3062) and (2924-2970) cm^{-1} due to $(C\text{-}H)_{aliph}$ and $(=C\text{-}H)_{Ar}$, respectively. The stretching vibrations of (C=O) for these compounds appeared as a strong bands at (1693-1624) cm^{-1}, while the stretching vibration of (C=C) appeared at (1620-1631) cm^{-1}.The stretching vibration of (C=N) of these compounds appeared at the range of (1550-1631) cm^{-1} while the stretching vibrations of (C-N) group appeared at (1203-1207) cm^{-1}. The (C-O) stretching vibrations appeared at the range of (1260-1319) cm^{-1}. Finally, the spectra show in addition to the above-mentioned bands, the bands of the bending vibrations of $(C\text{-}H)_{Ar}$ and $(C\text{-}H)_{Alph}$ [29-30].

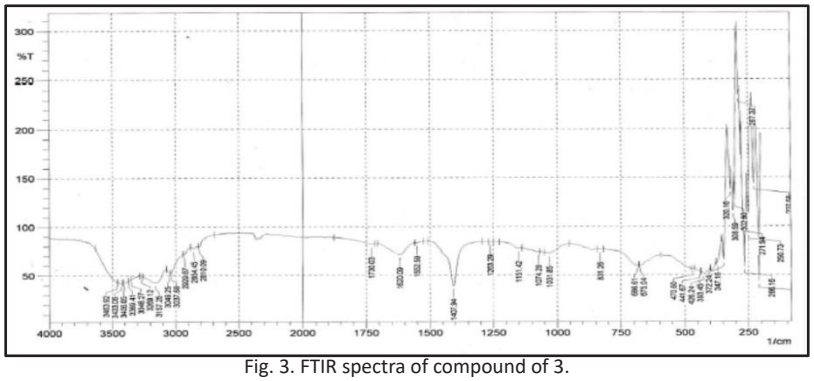

Fig. 3. FTIR spectra of compound of 3.

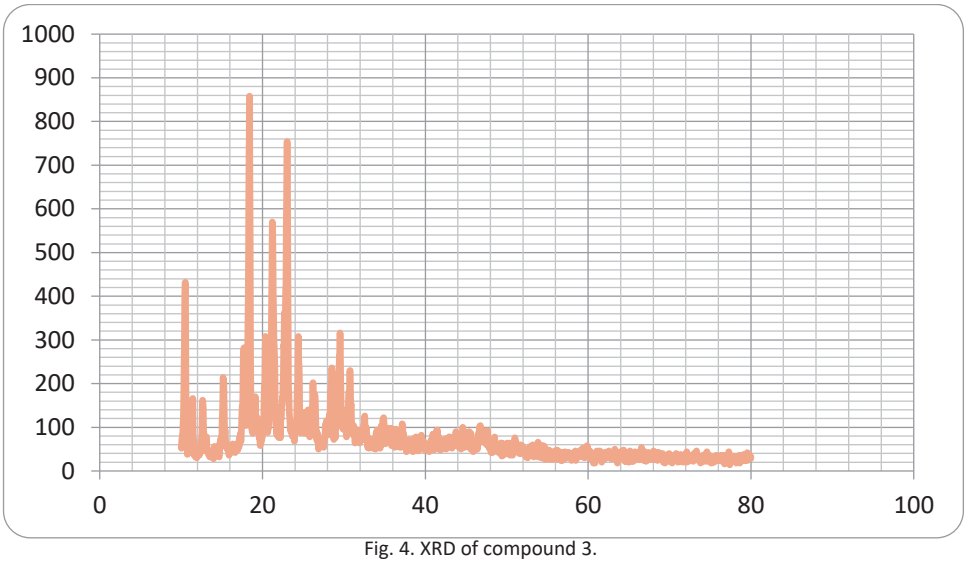

Fig. 4. XRD of compound 3.

XRD is a swift analytical technique common in characterizing crystal structures and an atomic spacing. Firstly, it is used for stage coincidence of a crystalline material and supplying information on unit cell dimensions. The XRD peaks are formed via deductive confusion of a monochromatic x-rays beam scattered at specified angles from every set of network planes in a sample. XRD has good potential for nano-structure analysis due to the width and shape of the reflections provide information about the material substructure, to determine the structure and crystal phase compound 3, 4, and the intensity was determined by step scanning 2θ range of (10-80°). The X-ray diffraction analysis of compound 4 nanoparticles is presented in Fig. 4. The diffraction peaks are located at 2θ = 21°, 32° and 44° in Fig. 4. Also, the X-ray diffraction analysis of Characteristic peaks have been observed in the XRD pattern at 2θ = 29°, 41° and 53°.in Fig. 5.

The Scanning Electron Microscopy (SEM)

The SEM is a one of kind of electron microscope that produces images of a specimen via scanning the sample surface by using a concentered beam of the electrons. The interaction between

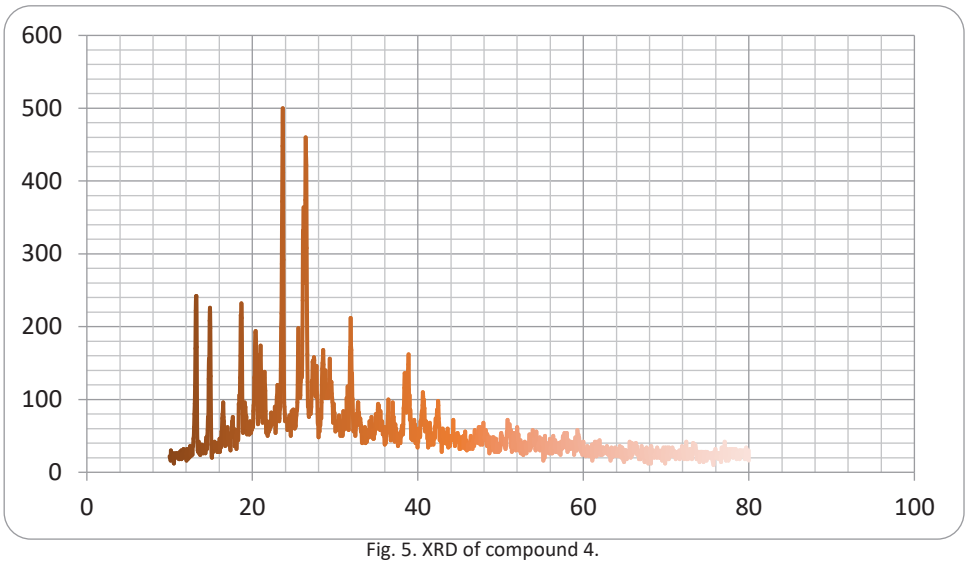

Fig. 5. XRD of compound 4.

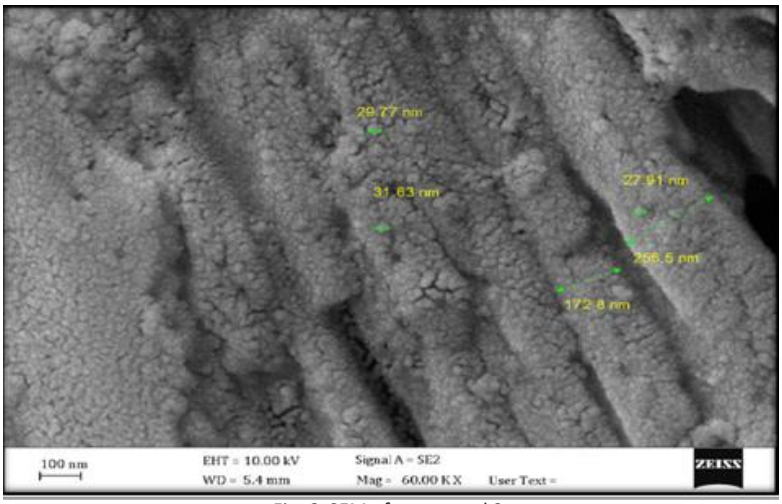

Fig. 6. SEM of compound 3.

electrons and atoms sample, leads to various signals which contain information on sample surface composition and topography. Fig. 6 shows the (SEM) images of Schiff base –g- kaempferol-coated Cu NPs, the SEM photographs that indicate the diameters of the particles with approximately (29 - 256 nm) diameters. Also, Fig. 7 shows the (SEM) images of Schiff base –g- kaempferol-coated Fe_3O_4NPs, that indicate the diameters of the particles approximately (35-46nm).

Atomic Force Microscopy (AFM)

This technique provides two and three-dimensional profiles of the surface at a nanoscale by measuring the forces between a sharp cantilever tip and a surface at a very short

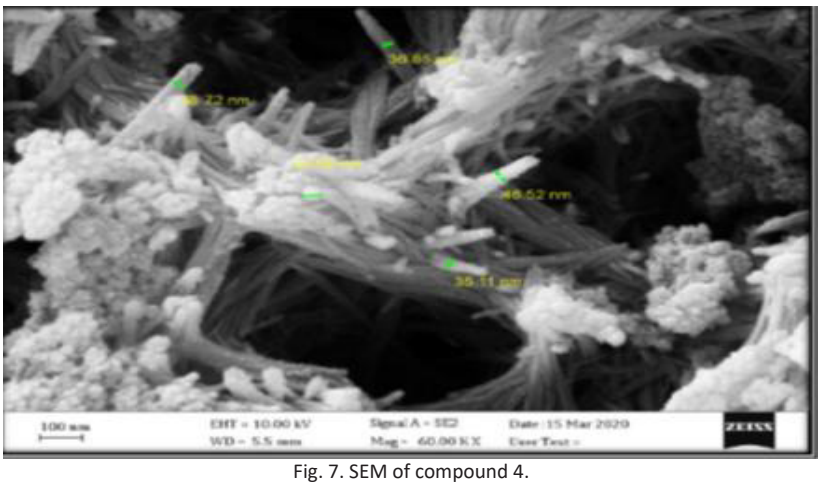

Fig. 7. SEM of compound 4.

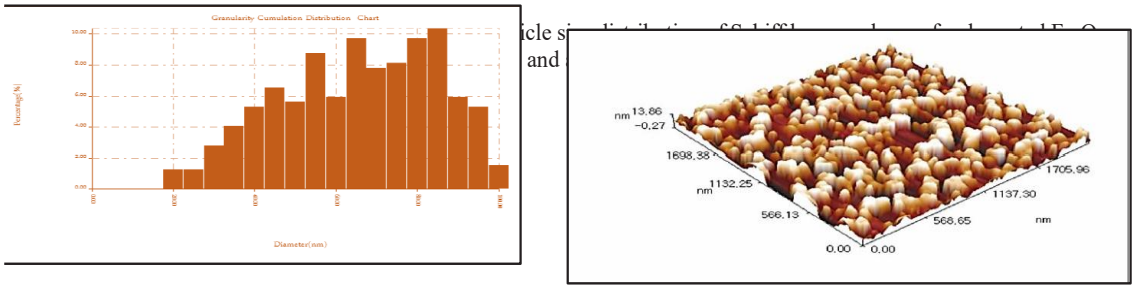

b a

Fig. 8. AFM three-dimensional image 3.b Granularity cumulation distribution of compound 3.

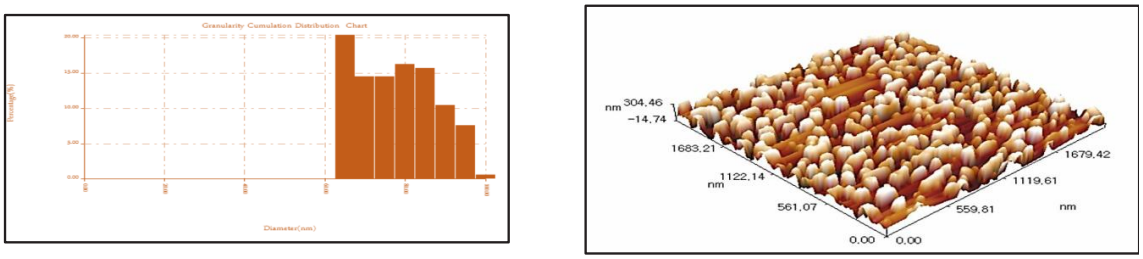

b a

Fig. 9. a) AFM three-dimensional image for compound 4 b) Granularity cumulation distribution for compound 4.

distance. Figs. 8 and 9 show the three-dimensional images of Schiff base –g- kaempferol coated of magnetite, copper and iron nanoparticles respectively, 10 and 11 show and display the granularity cumulation distribution charts for Schiff base –g- kaempferol -coated of magnetite, copper and iron nanoparticles respectively. Table 1 shows the particle size distribution of Schiff base –g- kaempferol -coated Cu NPs with a mean diameter range from 20-100 nm and an average diameter 62.99 nm. Table 2 shows the particle size distribution of Schiff base –g- kaempferol -coated Fe_3O_4 NPs with a mean diameter range from 65-100 nm and an average diameter 75.31 nm.

Antimicrobial Activity

Biological activates of some prepared compounds 1, 2, and 3 is tested against bacterial strains*, Rhizosporuim* using agar well diffusion method. The results shown in Table 3

Antibacterial activity of the prepared compounds was evaluated against types of bacteria (Gram-positive and Gram-negative), *Streptococcus, Bacillus, Escherichia coli, Klebsiella* the testing was performed using Agar diffusion method. The inhibition zone is measured by using a metric ruler over the inhibition zone, at its widest diameter, and then measuring from one edge of the zone to the other. It may be helpful to hold the

Table 1. Particle size distribution with an average diameter of Cu- Schiff base –g- kaempferol nanoparticles.

Avg. Diameter:6 2.99 nm			<=10% Diameter: 35.00nm					
<=50% Diameter:60.00 nm						<=90% Diameter:85.00 nm		
Diameter (nm)<	Volume (%)	Cumulation (%)	Diameter (nm)<	Volume (%)	Cumulation (%)	Diameter (nm)<	Volume (%)	Cumulation (%)
20.00	1.25	1.25	50.00	5.63	26.88	80.00	9.69	76.88
25.00	1.25	2.50	55.00	8.75	35.63	85.00	10.31	87.19
30.00	2.81	5.31	60.00	5.94	41.56	90.00	5.94	93.13
35.00	4.06	9.38	65.00	9.69	51.25	95.00	5.31	98.44
40.00	5.31	14.69	70.00	7.81	59.06	100.00	1.56	100.00
45.00	6.56	21.25	75.00	8.13	67.19	-	-	-

Table 2. Particle size distribution with an average diameter of Fe_2O_3- Schiff base –g- kaempferol nanoparticles.

Avg. Diameter:75.31 nm			<=10% Diameter:0 nm					
<=50% Diameter:75.00 nm						<=90% Diameter:85.00 nm		
Diameter (nm)<	Volume (%)	Cumulation (%)	Diameter (nm)<	Volume (%)	Cumulation (%)	Diameter (nm)<	Volume (%)	Cumulation (%)
65.00	20.35	20.35	80.00	16.28	65.70	95.00	7.56	99.42
70.00	14.53	34.88	85.00	15.70	81.40	100.00	0.58	100.00
75.00	14.53	49.42	90.00	10.47	91.86			

Table 3. Biological activates of prepared compounds 1, 2, and 3.

Comp.no	*Streptococcus (+ve)*	*Bacillus (+ve)*	*Escherichia coli (- ve)*	*Klebsiella (- ve)*	*Candida (fungus')*
1	10	15	13	18	23
2	4	18	14	11	12
3	----	----	4	3	6

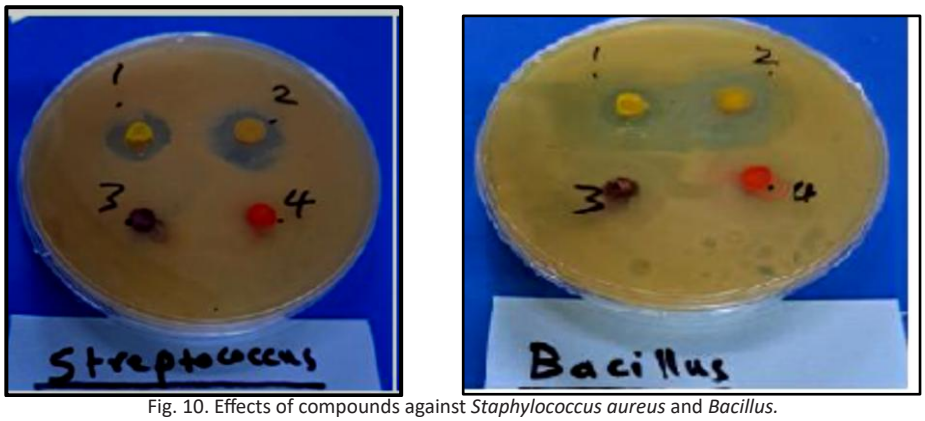

Fig. 10. Effects of compounds against *Staphylococcus aureus* and *Bacillus.*

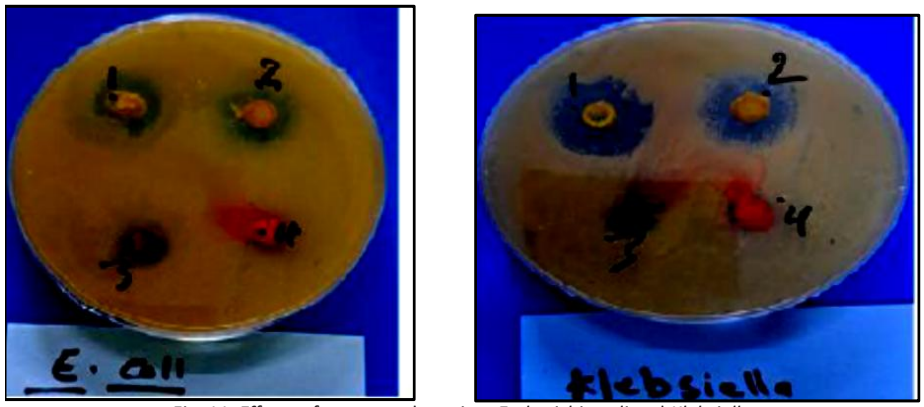

Fig. 11. Effects of compounds against *Escherichia coli* and *Klebsiella.*

panel up to the light and then use measurements in millimeters. Most of the tested compounds showed clear antibacterial activity, especially compound 1,2 the results of these two compounds were nearly similar to those of Ampicillin, which was used as a reference. Compound 5 showed the greatest activity against bacteria *Bacillus, Candida.* While compound **3** showed the strongest effect against *Candida* and both compounds had a strong effect against other bacteria (Figs. 10 and 11).

CONCLUSION

1-The present study aims to achieving synthesis, and characterization of some new chitosan\ kaempferol polymer

2- high molecular weights led to an increase in their biological activity

3-The prepared compounds proved to be resistant to some types of bacteria these compounds have medical application.

4- synthesis of new coated of chitosan -g- kaempferol nanoparticles of copper and iron.

CONFLICT OF INTEREST

The authors declare that there is no conflict of interests regarding the publication of this manuscript.

REFERENCES

1. Pohl F, Kong Thoo Lin P. The Potential Use of Plant Natural Products and Plant Extracts with Antioxidant Properties for the Prevention/Treatment of Neurodegenerative Diseases: In Vitro, In Vivo and Clinical Trials. Molecules. 2018;23(12):3283.
2. Holland TM, Agarwal P, Wang Y, Leurgans SE, Bennett DA, Booth SL, et al. Dietary flavonols and risk of Alzheimer dementia. Neurology. 2020;94(16).
3. Momeni HR, Kanje M. The calpain inhibitor VI prevents apoptosis of adult motor neurons. Neuroreport. 2005;16(10):1065-1068.
4. Kim S-H, Choi K-C. Anti-cancer Effect and Underlying Mechanism(s) of Kaempferol, a Phytoestrogen, on the

Regulation of Apoptosis in Diverse Cancer Cell Models. Toxicological Research. 2013;29(4):229-234.
5. Santos-Buelga C, González-Paramás AM, Oludemi T, Ayuda-Durán B, González-Manzano S. Plant phenolics as functional food ingredients. Advances in Food and Nutrition Research: Elsevier; 2019. p. 183-257. http://dx.doi.org/10.1016/bs.afnr.2019.02.012
6. Fan Z-F, Ho S-T, Wen R, Fu Y, Zhang L, Wang J, et al. Design, Synthesis and Molecular Docking Analysis of Flavonoid Derivatives as Potential Telomerase Inhibitors. Molecules. 2019;24(17):3180.
7. Azizi A. Green Synthesis of Fe3O4 Nanoparticles and Its Application in Preparation of Fe_3O_4/Cellulose Magnetic Nanocomposite: A Suitable Proposal for Drug Delivery Systems. Journal of Inorganic and Organometallic Polymers and Materials. 2020;30(9):3552-3561.
8. Qu J, Liu G, Wang Y, Hong R. Preparation of Fe_3O_4–chitosan nanoparticles used for hyperthermia. Adv Powder Technol. 2010;21(4):461-467.
9. Lourenço IM, Pelegrino MT, Pieretti JC, Andrade GP, Cerchiaro G, Seabra AB. Synthesis, characterization and cytotoxicity of chitosan-coated Fe_3O_4 nanoparticles functionalized with ascorbic acid for biomedical applications. Journal of Physics: Conference Series. 2019;1323(1):012015.
10. Piosik E, Klimczak P, Ziegler-Borowska M, Chełminiak-Dudkiewicz D, Martyński T. A detailed investigation on interactions between magnetite nanoparticles functionalized with aminated chitosan and a cell model membrane. Materials Science and Engineering: C. 2020;109:110616.
11. Abdulghani AJ, Al-Ogedy WM. Synthesis and Characterization of Multishapes of Fe_3O_4 Nanoparticle by Solve-Hydrothermal Method Using Microwave Radiation. Baghdad Science Journal. 2016;13(2):0331.
12. Yew YP, Shameli K, Miyake M, Ahmad Khairudin NBB, Mohamad SEB, Naiki T, et al. Green biosynthesis of superparamagnetic magnetite Fe_3O_4 nanoparticles and biomedical applications in targeted anticancer drug delivery system: A review. Arabian Journal of Chemistry. 2020;13(1):2287-2308.
13. Priyadarshana G, Kottegoda N, Senaratne A, de Alwis A, Karunaratne V. Synthesis of Magnetite Nanoparticles by Top-Down Approach from a High Purity Ore. Journal of Nanomaterials. 2015;2015(1).
14. Zhu N, Ji H, Yu P, Niu J, Farooq MU, Akram MW, et al. Surface Modification of Magnetic Iron Oxide Nanoparticles. Nanomaterials. 2018;8(10):810.
15. Ali A, Zafar H, Zia M, ul Haq I, Phull AR, Ali JS, et al. Synthesis, characterization, applications, and challenges of iron oxide nanoparticles. Nanotechnology, Science and Applications. 2016;Volume 9:49-67.
16. Kumar P, Khanduri H, Pathak S, Singh A, Basheed GA, Pant RP. Temperature selectivity for single phase hydrothermal synthesis of PEG-400 coated magnetite nanoparticles. Dalton Transactions. 2020;49(25):8672-8683.
17. Wallyn J, Anton N, Vandamme TF. Synthesis, Principles, and Properties of Magnetite Nanoparticles for In Vivo Imaging Applications—A Review. Pharmaceutics. 2019;11(11):601.
18. Majidi S, Zeinali Sehrig F, Farkhani SM, Soleymani Goloujeh M, Akbarzadeh A. Current methods for synthesis of magnetic nanoparticles. Artificial Cells, Nanomedicine, and Biotechnology. 2014;44(2):722-734.
19. Rubina MS, Vasil'kov AY, Naumkin AV, Shtykova EV, Abramchuk SS, Alghuthaymi MA, et al. Synthesis and characterization of chitosan–copper nanocomposites and their fungicidal activity against two sclerotia-forming plant pathogenic fungi. Journal of Nanostructure in Chemistry. 2017;7(3):249-258.
20. Muthukrishnan AM. Green Synthesis of Copper-Chitosan Nanoparticles and Study of its Antibacterial Activity. Journal of Nanomedicine and Nanotechnology. 2015;06(01).
21. New technologies, new systems, new rules. United Nations Publications; 2002. http://dx.doi.org/10.18356/244d73c7-en
22. Pawar HA, Gavasane AJ, Choudhary PD. A Novel and Simple Approach for Extraction and Isolation of Curcuminoids from Turmeric Rhizomes. Advances in Recycling and Waste Management. 2018;06(01).
23. Saeed RS, Hussein FA, Awad SH, Al-rawi MS. Synthesis and Study Antibacterial Activity of Some New Polymers Containing Maleimide Group. Journal of Physics: Conference Series. 2021;1879(2):022070.
24. Kapilraj N, Sithambaresan M, Mathiventhan U. Synthesis and Characterization of Copper(II) Complexes of Salicylaldehyde Semicarbazone and 1,10 Phenanthroline and their Antibacterial Activities. International Journal of Scientific and Engineering Research. 2018;9(7):940-946.
25. Awad SH, Yousif SA, Mahmood WAR, Mahmood TA. Synthesis and characterization of chitosan-G-phthalic anhydride with different drugs. AIP Conference Proceedings: AIP Publishing; 2020. p. 020028.
26. Patel AK, Patel PS. Design, Synthesis and Microbicidal Activity of New Series Schiff Base Derivatives. Biochemical And Cellular Archives. 2024;24(1).
27. Wulandari IO, Mardila VT, Santjojo DJDH, Sabarudin A. Preparation and Characterization of Chitosan-coated Fe_3O_4 Nanoparticles using Ex-Situ Co-Precipitation Method and Tripolyphosphate/Sulphate as Dual Crosslinkers. IOP Conference Series: Materials Science and Engineering. 2018;299:012064.
28. Gandhi H, Khan S. Biological Synthesis of Silver Nanoparticles and Its Antibacterial Activity. Journal of Nanomedicine and Nanotechnology. 2016;07(02).
29. Tengroth C, Gasslander U, Andersson FO, Jacobsson SP. Cross-Linking of Gelatin Capsules with Formaldehyde and Other Aldehydes: An FTIR Spectroscopy Study. Pharmaceutical Development and Technology. 2005;10(3):405-412.
30. Fan QG, Lewis DM, Tapley KN. Characterization of cellulose aldehyde using Fourier transform infrared spectroscopy. J Appl Polym Sci. 2001;82(5):1195-1202.
31. Hirai A, Odani H, Nakajima A. Determination of degree of deacetylation of chitosan by 1H NMR spectroscopy. Polym Bull. 1991;26(1):87-94.
32. Abdulsada ZS, Hassan SS, Awad SH. Synthesis, Characterization and Biological Activity of New Oleander Complexes against Bacteria Found in Polluted Water. Indonesian Journal of Chemistry. 2023;23(6):1638.
33. Chavan SS, Sawant VA. Synthesis, structural characterization, thermal and electrochemical studies of Mn(II), Co(II), Ni(II) and Cu(II) complexes containing thiazolylazo ligands. J Mol Struct. 2010;965(1-3):1-6.
34. Kang N, Xu YZ, Cai YL, Li WH, Weng SF, Feng W, et al. Different states in orthorhombic crystalline phase of high-density polyethylene. J Mol Struct. 2001;562(1-3):19-24.